



**HAL**  
open science

## **Agr system of *Listeria monocytogenes* EGD-e: role in adherence and differential expression pattern.**

Aurélie Rieu, Stéphanie Weidmann, Dominique Garmyn, Pascal Piveteau,  
Jean Guzzo

### ► **To cite this version:**

Aurélie Rieu, Stéphanie Weidmann, Dominique Garmyn, Pascal Piveteau, Jean Guzzo. Agr system of *Listeria monocytogenes* EGD-e: role in adherence and differential expression pattern.. Applied and Environmental Microbiology, 2007, 73 (19), pp.6125-33. 10.1128/aem.00608-07 . hal-00441284

**HAL Id: hal-00441284**

**<https://hal.science/hal-00441284>**

Submitted on 15 Dec 2009

**HAL** is a multi-disciplinary open access archive for the deposit and dissemination of scientific research documents, whether they are published or not. The documents may come from teaching and research institutions in France or abroad, or from public or private research centers.

L'archive ouverte pluridisciplinaire **HAL**, est destinée au dépôt et à la diffusion de documents scientifiques de niveau recherche, publiés ou non, émanant des établissements d'enseignement et de recherche français ou étrangers, des laboratoires publics ou privés.

1                                   **The *agr* system of *L. monocytogenes* EGD-e :**  
2                                   **role in adherence and differential expression pattern**  
3

4   Running title: *agr* mutation in biofilm formation of *L. monocytogenes*

5   Aurélie Rieu<sup>1</sup>, Stéphanie Weidmann<sup>2</sup>, Dominique Garmyn<sup>1</sup>, Pascal Piveteau<sup>1\*</sup> and Jean  
6   Guzzo<sup>2</sup>

7   <sup>1</sup>*UMR 1229 Microbiologie du Sol et de l'Environnement (MSE), Université de Bourgogne,*  
8   *INRA, F-21000 Dijon, France*

9   <sup>2</sup>*Laboratoire Recherche en Vigne et Vin (REVV), Université de Bourgogne, IUVV, F-21000*  
10   *Dijon, France*

11   \* Corresponding author : Pascal Piveteau Phone: + 33 3 80 39 68 93. Fax : + 33 3 80 39 39 55.

12   E-mail : [piveteau@u-bourgogne.fr](mailto:piveteau@u-bourgogne.fr)

13

14

15 **ABSTRACT**

16

17 In this study, we investigated the *agrBDCA* operon in the pathogenic bacterium *Listeria*  
18 *monocytogenes* EGD-e. In-frame deletion of *agrA* and *agrD* resulted in an altered adherence  
19 and biofilm formation on abiotic surfaces, suggesting the involvement of the *agr* system of *L.*  
20 *monocytogenes* during the early stages of biofilm formation. Real time PCR experiments  
21 indicated that the transcript levels of *agrBDCA* depended on the stage of biofilm  
22 development, since it was lower after initial attachment period than during biofilm growth.  
23 Whereas, during planktonic growth, transcription was not growth-phase dependent. The  
24 mRNA quantification data also suggested that the *agr* system was autoregulated and pointed  
25 to a differential expression of the *agr* genes during sessile and planktonic growth. Although  
26 the RT-PCR experiments revealed that the four genes were transcribed as a single messenger,  
27 chemical half-life and 5' RACE experiments indicated that the full size transcript underwent  
28 cleavage followed by degradation of the *agrC* and *agrA* transcripts, which supposes a  
29 complex regulation of *agr* transcription.

30

31

## 32 INTRODUCTION

33

34 *Listeria monocytogenes* is a Gram-positive human pathogenic bacterium ; it is the causative  
35 agent of listeriosis, a serious infection characterized by high mortality rates, in  
36 immunocompromised individuals and pregnant women (19). This pathogenic bacterium is  
37 widely spread in the environment (soil, vegetation, animals, farm environment). In connexion  
38 with these extended reservoirs, *L. monocytogenes* is also a contaminant of the food industry.  
39 Its presence on working surfaces in food-processing plants is a major problem as a source of  
40 food contamination (1, 32). As most bacteria, *L. monocytogenes* is able to colonize surfaces  
41 and form biofilms (sessile growth) while, in natural environments, free floating cells  
42 (planktonic growth) are transitory (28). Several steps can be identified during biofilm  
43 development : after an initial step of reversible then irreversible adherence, bacteria grow as  
44 microcolonies and spread on the surface ; finally, biofilms develop as complex, three-  
45 dimensional structures during the maturation step (17). Biofilm development and maturation  
46 requires complex cellular mechanisms in which cell-cell communication is involved (14, 30).  
47 To date, three major signalling systems have been identified ; to regulate these systems,  
48 bacterial extracellular signalling molecules called autoinducers are produced (8). The  
49 acylhomoserine lactones (AHL) have been identified as autoinducers in Gram-negative  
50 bacteria (3, 13, 27, 46). The autoinducer 2 (AI-2) is found in both Gram-negative and Gram-  
51 positive bacteria (5, 7, 11, 35, 36, 54). Finally, peptide-mediated signalling pathways have  
52 been characterized in Gram-positive bacteria. Among these, the *agr* system has been  
53 described initially in *Staphylococcus aureus* (41) ; the production of many of its virulence  
54 factors (toxins, enzymes and cell surface proteins) is regulated by this system (4). The role of  
55 the *agr* system during *S. aureus* biofilm development is complex (57). It depends on the  
56 hydrodynamic conditions of the experimental set up ; under static conditions, *agr* expression

57 reduces the attachment of the cells to the surface (52, 55) and under turbulent dynamic  
58 conditions, *agr* expression may affect biofilm maturation (55). Orthologs of the *agr* system  
59 have also been described in *Enterococcus faecalis* (*fsr*) (45), *Lactobacillus plantarum* (*lam*)  
60 (48) and *L. monocytogenes* (*agr*) (6). In *E. faecalis*, expression of a gelatinase (GelE) is *fsr*  
61 dependent (45). In *L. plantarum*, the *lam* system plays a role during biofilm development  
62 (48).

63 In *L. monocytogenes*, the four genes (*agrB*, *agrD*, *agrC* and *agrA*) of the *agr* locus are  
64 organized as an operon (Fig. 1A). They encode the two-component histidine kinase AgrC and  
65 response regulator AgrA, a precursor peptide AgrD and AgrB, a protein that is involved in the  
66 processing of AgrD into a matured autoinducing peptide. Limited data concerning the role of  
67 the *agr* locus on the physiology of *L. monocytogenes* is available. Williams *et al.* (53) showed  
68 that among sixteen putative response regulator genes of *L. monocytogenes* EGD-e, in-frame  
69 deletion in *agrA* did not affect the growth in BHI medium at various temperatures (20°C,  
70 37°C and 43°C), in the presence of 9% NaCl, 5% ethanol or 0.025% H<sub>2</sub>O<sub>2</sub>. Swimming  
71 motility was not affected either. No alteration of virulence could be identified during *in vitro*  
72 infection of cell cultures nor *in vivo* after intravenous infection of BALB/c mice. In a previous  
73 study, Autret *et al.* (6) reported a moderate attenuation of the virulence in Swiss mice after  
74 insertion of Tn1545 in the *L. monocytogenes* EGD-e *agrA* gene.

75 To further elucidate the role of the *agr* system, we first of all examined its involvement during  
76 attachment to abiotic surfaces and biofilm growth. *agrA* and *agrD* in-frame deletion mutants  
77 were compared to the parental strain EGD-e during sessile growth. Secondly, we determined  
78 the expression pattern of the four genes of the *agr* operon during planktonic and sessile  
79 growth and we evidenced post-transcriptional events during expression of this operon.

80

81

## 82 MATERIALS AND METHODS

83

### 84 Bacterial strains and growth media

85 The bacterial strains and plasmids used in this study and their characteristics are shown in  
86 Table 1. *L. monocytogenes* EGD-e, isolated from a rabbit listeriosis outbreak (39), and two  
87 mutants, derivatives of *L. monocytogenes* EGD-e, *L. monocytogenes* DG119D ( $\Delta agrD$ ) and *L.*  
88 *monocytogenes* DG125A ( $\Delta agrA$ ) were grown in tryptic soy broth (TSB, Biokar diagnostics,  
89 Pantin, France) at 25°C for biofilm and planktonic cultures and in brain heart infusion broth  
90 (BHI, Biokar diagnostics) at 40°C for mutant construction. *Escherichia coli* TOP10 and  
91 Match1 (Invitrogen, Cergy Pontoise, France) were grown aerobically in Luria-Bertani broth  
92 (LB, Biokar diagnostics) at 37°C. When appropriate, antibiotics (Sigma, St Quentin Fallavier,  
93 France) were added as follows: kanamycin, 50  $\mu\text{g}\cdot\text{ml}^{-1}$  (*E. coli*); ampicillin, 200  $\mu\text{g}\cdot\text{ml}^{-1}$  (*E.*  
94 *coli*); chloramphenicol, 10  $\mu\text{g}\cdot\text{ml}^{-1}$  (*L. monocytogenes*) (Table 1).

### 95 In-frame deletion of *agrD* and *agrA* genes

96 The mutant strains listed in Table 1, carrying an in-frame deletion in the response regulator  
97 *agrA* or in the precursor peptide *agrD* genes, were constructed from the parental strain *L.*  
98 *monocytogenes* EGD-e using a two step integration/excision procedure (10) which is based on  
99 the mutagenesis plasmid pGF-EM (33).  
100 First, for the construction of an *agrA* in-frame deletion mutant, primers C13 and A12 (Table  
101 2) were used to amplify a 600-bp DNA fragment including the 3' end of *agrC* and the ATG of  
102 *agrA*. The PCR product was cloned into pGF-EM (33) after digesting this PCR product and  
103 vector with HindIII/XbaI. The resulting plasmid, pGID121 was transformed into chemically  
104 competent *E. coli* Match1 as recommended by the manufacturer (Invitrogen). Primers A15  
105 and E2 (Table 2) were used to amplify a 500-bp internal fragment of *agrA*. The resulting  
106 fragment was cloned into pCR2.1 TOPO vector (Invitrogen) to obtain plasmid pGID118. This

107 vector was transferred into *E. coli* TOP10. Plasmid pGID118 was digested with NheI/EcoRI  
108 and the resulting 500-bp fragment containing an internal part of *agrA* was ligated into  
109 pGID121 restricted with XbaI/EcoRI to obtain pGID125. This plasmid was electroporated  
110 into *L. monocytogenes* EGD-e.

111 Secondly, a similar strategy was used for the construction of an *agrD* in-frame deletion  
112 mutant. Primers D1 and D2 (Table 2) were used to amplify a 400-bp DNA fragment including  
113 the 5' end of *agrD*. The PCR product was cloned into pGF-EM (33) to obtain pGID112.  
114 Primers D3 and D4 (Table 2) were used to amplify a 600-bp DNA fragment including the 3'  
115 end of *agrD* and the 5' end of *agrC*. The resulting fragment was cloned into pCR2.1 TOPO  
116 vector (Invitrogen) to obtain plasmid pGID109. After digestion, the plasmid pGID109 was  
117 ligated into digested plasmid pGID112 to obtain pGID119. This plasmid was electroporated  
118 into *L. monocytogenes* EGD-e.

119 Finally, transformants were selected on BHI agar plates (Biokar diagnostics) containing 10  
120  $\mu\text{g.ml}^{-1}$  chloramphenicol (Sigma). A transformant was serially subcultured in BHI at 40°C to  
121 direct chromosomal integration of the plasmid by homologous recombination. Chromosomal  
122 integration was confirmed by PCR and a single colony, with a chromosomal integration, was  
123 serially subcultured in BHI at 40°C and screened for loss of chloramphenicol resistance.  
124 Allelic exchange mutagenesis was confirmed by PCR amplification and direct sequencing of  
125 the PCR product (GENOME express, Meylan, France). The mutants selected were named  
126 DG125A ( $\Delta\text{agrA}$ ) and DG119D ( $\Delta\text{agrD}$ ). The deletion of 106 bp in strain DG125A ( $\Delta\text{agrA}$ )  
127 (Fig. 1B) and the deletion of 49 bp in strain DG119D ( $\Delta\text{agrD}$ ) (Fig. 1C) resulted in a  
128 frameshift causing the premature appearance of a stop codon and thus the premature stop of  
129 translation.

130 **Adhesion on glass slide**

131 An overnight culture of the bacterium in TSB was used to inoculate (1/100, vol/vol) fresh  
132 TSB and was grown at 25°C to an optical density at 600 nm of 0.1. Five microliters of the  
133 culture to be tested was then deposited on a glass slide, and the glass slide was incubated for 2  
134 hours at 25°C. After incubation, the glass slide was washed twice in distilled water and the  
135 adhering cells were stained with a 0.1% (wt/vol) aqueous crystal violet solution for one  
136 minute and washed with distilled water. Adhering cells were observed using a ZEISS  
137 Axioplan 2 imaging microscope. For each experiment, 12 replicates resulting from three  
138 independent inocula were analysed.

### 139 **Biofilm formation**

140 **(i) on polystyrene microplate** An overnight culture of the bacterium in TSB at 25°C was  
141 used to inoculate (1/100, vol/vol) fresh TSB. One hundred microliters per well were  
142 dispensed on a 96 well microtiter plate (Nunc, Dominique Dutscher S.A., Brumath, France)  
143 which was incubated at 25°C for 16 to 72 h. Cells attached to the well walls were quantified  
144 as previously described (16) with some modifications. After incubation, the medium was  
145 removed from each well, and the plates were washed twice using a microtiter plate washer  
146 (Cellwash; Thermolabsystems, Cergy Pontoise, France) with 100 µl of 150 mM NaCl  
147 solution in order to remove loosely attached cells. The plates were then stained with a 0.05%  
148 (wt/vol) aqueous crystal violet solution for 45 min and washed three times. In order to  
149 quantitatively assess biofilm production, 100 µl of 96% ethanol (vol/vol) were added to each  
150 well, and the optical density at 595 nm was determined. For each experiment, 15 replicates  
151 resulting from three independent inocula were analysed. Each microtiter plate included eight  
152 wells with sterile TSB as control.

153 **(ii) on stainless steel chips** AISI 304 stainless steel chips of 8 cm diameter (Goodfellow  
154 SARL, Lille, France) were inserted in Petri dishes containing 20 mL of inoculated TSB  
155 (1/100, vol/vol) and incubated at 25°C for 2 h to allow adhesion. For biofilm development,

156 the medium was removed and 20 mL of fresh TSB was added. Biofilms were grown during  
157 24 h and 72 h at 25°C. Following incubation, the medium was removed and 10 ml of saline  
158 solution (150 mM NaCl) were softly poured twice onto coupons and agitated 1 min on an  
159 orbital shaker at 240 rpm (IKA®KS 130 basic) to remove loosely adhering bacteria. Sessile  
160 cells were detached from coupons in 10 ml saline solution by scraping with a sterile  
161 disposable cell lifter (TPP, Dominique Dutscher S.A.).

#### 162 **RNA extraction and cDNA preparation**

163 Cells were harvested by centrifugation (10000g 5 min), resuspended in 1 ml of Tri-reagent  
164 (Sigma) and disrupted with glass beads (106 µm) in a FastPrep FP120 Instrument (Thermo  
165 Savant-BIO101) at 4°C for 8x30s at 6000g. Nucleic acids were extracted twice in 0.2 volume  
166 of chloroform and purified by precipitation in 1 volume of isopropanol. RNA pellets were  
167 dried and resuspended in 80 µl of RNase-free water. Nucleic acid concentrations were  
168 calculated by measuring absorbance at 260 nm using a SmartSpec Plus Spectrophotometer  
169 (Bio-Rad, Marnes La Coquette, France).

170 Before reverse transcription, 2 µg of total RNA were treated with 2 U of DNase (Invitrogen)  
171 as described by the manufacturer. The absence of chromosomal DNA contamination was  
172 checked by real-time PCR. cDNA were then synthesized using an iScript cDNA synthesis kit  
173 (Bio-Rad) as recommended.

#### 174 **Real time PCR experiments**

175 Real time PCR as described by Desroche *et al.* (15) was used to quantify mRNA levels. Gene-  
176 specific primers (Table 2, Fig. 1A) were designed to amplify cDNAs of the transcripts of  
177 *agrB*, *agrD*, *agrC* and *agrA* with the Bio-Rad SYBR Green kit in a Bio-Rad I-Cycler. These  
178 gene-specific primers were designed outside zones of deletion allowing the determination of  
179 the transcript levels of the *agrB*, *agrD*, *agrC* and *agrA* genes in the parental strain and in both  
180 mutants DG125A ( $\Delta agrA$ ) and DG119D ( $\Delta agrD$ ). This method was used to analyse their

181 mRNA level during planktonic growth at early exponential phase ( $6.5 \cdot 10^7$  cfu.ml<sup>-1</sup> ; OD<sub>600</sub> of  
182 0.1), mid-exponential phase ( $2.5 \cdot 10^8$  cfu.ml<sup>-1</sup> ; OD<sub>600</sub> of 0.4) and stationary phase ( $4 \cdot 10^8$   
183 cfu.ml<sup>-1</sup> ; OD<sub>600</sub> of 0.6) and after 2 h, 24 h and 72 h of biofilm formation on AISI 304  
184 stainless steel chips. The specificity of each primer pair was controlled by melt curves, and  
185 the mean of efficiencies for the five primer pairs was 98±9%. Results were analysed using the  
186 comparative critical threshold method ( $\Delta\Delta C_T$ ) in which the amount of targeted mRNA was  
187 first of all normalised using a specific mRNA standard, then compared to a calibrator  
188 condition (15). *drm*, a gene coding for a phosphopentomutase was selected as internal  
189 standard since *drm* transcript levels were stable in the conditions tested. For our work, the  
190 calibrator condition corresponded to *agrA* mRNA level at OD<sub>600</sub> of 0.1. The relative level of  
191 *agrA* mRNA at OD<sub>600</sub> of 0.1 thus corresponded to 1. mRNA quantification was performed in  
192 triplicate from total RNA extracted from three independent cultures.

### 193 **RT-PCR**

194 RT-PCR were performed with cDNA synthesized with total RNA extracted from three  
195 different mid-exponential phase cultures (OD<sub>600</sub> of 0.4) as described above. Specific primers  
196 (Table 2) were designed to amplify transcripts of the four genes and the two intergenic  
197 regions. PCR products were separated by electrophoresis on a 1% agarose gel (Invitrogen).  
198 Samples were checked for DNA contamination by performing PCR prior reverse  
199 transcription.

### 200 **Northern blotting**

201 Northern blot analysis were performed by fractionation of RNA samples on 1% (wt/vol)  
202 agarose gel containing 20% (wt/vol) formaldehyde. 30 µg of total RNA were loaded in each  
203 well of the gel. Transfer to a nylon membrane (Hybond-N, Amersham, Orsay, France) was  
204 performed as recommended. Internal probes (Fig. 1A) of the *agrB*, *agrC* and *agrA* genes were  
205 generated by PCR using primers described in Table 2. 10 ng of PCR products were labelled

206 with [ $\alpha$ -<sup>32</sup>P]dATP (Amersham) by the random priming method according to the manufacturer  
207 instructions (Invitrogen) to produce specific RNA probes. Sizes were determined with a RNA  
208 ladder (Invitrogen) as molecular weight standard.

### 209 **mRNA chemical half-life determination**

210 The chemical half-life of mRNA of the 4 genes of the *agr* operon was determined from mid-  
211 exponential phase cultures (OD<sub>600</sub> of 0.4). Total RNA was isolated as described above from  
212 samples taken 1, 4, 7 and 10 min after rifampicin treatment (250  $\mu$ g.ml<sup>-1</sup>, Sigma). The half-  
213 life was determined for each gene by real-time PCR using the time at which rifampicin was  
214 added as calibrator and 16S rRNA transcript levels as internal standard.

### 215 **Analysis of the 5' end of *agr* mRNA**

216 Primer extensions were performed by incubating 5  $\mu$ g of RNA isolated from *L.*  
217 *monocytogenes* cells in planktonic growth, 20 pmol of oligonucleotide, 92 GBq of [ $\alpha$ -  
218 <sup>32</sup>P]dATP (Perkin-Elmer, Courtaboeuf, France) and 100 U of SuperScriptII reverse  
219 transcriptase (Invitrogen). The oligonucleotides used in this experiment are described in Table  
220 2. The corresponding DNA-sequencing reactions were carried out using the same primers and  
221 Cycle Reader<sup>TM</sup> DNA Sequencing Kit as recommended by the manufacturer (Fermentas,  
222 Euromedex, Souffel Weysersheim, France).

223 A capping assay was used to distinguish 5' triphosphate (indicating initiation points) from 5'  
224 monophosphate (indicating processed products) according to Bensing *et al.* (9), using the 5'  
225 RACE kit (Ambion, Applied Biosystems, Courtaboeuf, France). Only 5' monophosphate are  
226 selectively ligated to an RNA oligonucleotide. The primary 5' end may be ligated only after  
227 removal of a 5' pyrophosphate through Tobacco Acid Pyrophosphatase (TAP) activity. The  
228 oligonucleotides used in this experiment are described in Table 2. Sequencing of 5'-RACE  
229 products obtained from TAP-treated and non-treated RNA was performed to differentiate  
230 cleavage products from primary transcripts. Primers used for PCR amplification between

231 adaptor and the gene of interest are described in Table 2. PCR products were sequenced by  
232 GENOME express.

### 233 **Statistical analysis**

234 A one-way analysis of variance (ANOVA) was performed using the SigmaStat® Version  
235 3.0.1 software (SPSS Inc.) in order to test the significance of the differences (i) in gene  
236 expression during planktonic growth and biofilm formation using  $\Delta C_T$  value and (ii) in  
237 biofilm quantity. When one-way ANOVA was significant, the Holm-Sidak test ( $n=3$ ,  $P<0.05$ )  
238 was used to locate significant differences.

### 239 **Nucleotide sequence accession number**

240 The DNA sequence data of the mutant strains described in this work have been deposited in  
241 the GenBank/EMBL/DDBJ under the following accession numbers: AM412557 and  
242 AM412558

243

244

245 **RESULTS**

246

247 **The *agr* operon is involved during the sessile growth of *L. monocytogenes* EGD-e**

248 In order to study the involvement of the putative transcriptional regulator AgrA during sessile  
249 growth, an *agrA* in-frame deletion mutant of *L. monocytogenes* EGD-e was constructed. As  
250 expected, this mutation did not alter cell or colony morphology nor planktonic growth (data  
251 not shown). In contrast, mutant DG125A ( $\Delta$ *agrA*) was affected on glass slide adherence.  
252 Indeed, the number of adhered cells of DG125A was significantly reduced (n=3, P<0.05) by  
253 62% compared to the parental strain EGD-e (Fig. 2A). As cell-cell communication affects  
254 biofilm formation in many bacterial species, an *agrD* in-frame deletion was designed to  
255 generate a mutant unable to produce the putative autoinducer peptide processed from AgrD.  
256 As demonstrated in mutant DG125A ( $\Delta$ *agrA*), no pleiotropic effect was observed in mutant  
257 DG119D ( $\Delta$ *agrD*) (data not shown). Moreover, the adhesion phenotype of DG119D ( $\Delta$ *agrD*)  
258 was similar to that of DG125A ( $\Delta$ *agrA*) (Fig. 2A). Micrographs of the microscopic field of  
259 adhering cells on glass slides confirmed that the quantity of adhering cells with *L.*  
260 *monocytogenes* DG119D ( $\Delta$ *agrD*) and DG125A ( $\Delta$ *agrA*) was less compared to the parental  
261 strain EGD-e (Fig. 2B). These results suggested the involvement of the *agr* system during  
262 adhesion of *L. monocytogenes*, the first step in biofilm development.

263 The ability of *L. monocytogenes* EGD-e to develop biofilms on polystyrene was also affected  
264 by the deletion of *agrA* and *agrD* (Fig. 3). Indeed, there was significantly less biofilm (n=3,  
265 P<0.05) produced within the first 24 h of incubation. The differences were no longer  
266 significant during the later stages of biofilm formation, namely, at 48 h and 72 h.

267 In light of the sessile growth alteration observed in the mutants with deletion in the genes  
268 encoding the putative transcriptional regulator AgrA and the putative autoinducer peptide  
269 processed from AgrD, we therefore decided to investigate the expression of the *agr* operon

270 during sessile and planktonic growth.

### 271 **Relative expression and transcriptional autoregulation of the genes of the *agr* operon**

272 The transcription of the four genes of the *agr* operon was studied during sessile and  
273 planktonic growth using real time PCR experiments with each of the four primer sets (Fig.  
274 1A, Table 2, b [BF2-BR2] ; d [DF2-DR2] ; c [CF2-CR2] ; a [AF2-AR2]). Analysis of the  
275 relative expression levels indicated that, during sessile growth, the levels of transcripts of  
276 *agrB*, *agrD* and *agrC* were significantly lower (n=3, P<0.05) after 2 h of adhesion than after  
277 24 h and 72 h of sessile growth (Fig. 4A). For each gene, the differences of relative  
278 expression observed between 24 h and 72 h of biofilm growth were not significant. The levels  
279 of *agrA* transcripts were similar at 2 h, 24 h and 72 h. Furthermore, during sessile growth, for  
280 each condition, the levels of transcripts of *agrB*, *agrD* and *agrC* were never significantly  
281 different. In contrast, the relative expression levels of *agrA*, for each condition, were  
282 significantly lower (n=3, P<0.05) than those of *agrB*, *agrD* and *agrC*.

283 During planktonic growth, the relative expression levels of each gene was not affected by the  
284 phase of growth. The levels of transcripts of *agrB* and *agrD*, for each condition, were never  
285 significantly different. In contrast, the relative expression levels of *agrC* and *agrA*, for each  
286 condition, were significantly lower (n=3, P<0.05) than those of *agrB* and *agrD*. For example,  
287 under our experimental conditions, at mid exponential growth phase (OD<sub>600nm</sub> of 0.4) *agrC*  
288 and *agrA* transcript levels were respectively of 13 and 24 fold lower than the *agrB* transcript  
289 level (Fig. 4A).

290 The relative expression levels of the four genes of the *agr* operon were determined at mid-  
291 exponential phase during planktonic growth (OD<sub>600</sub> of 0.4) in the parental and mutant ( $\Delta$ *agrA*,  
292  $\Delta$ *agrD*) backgrounds. In mutant DG125A ( $\Delta$ *agrA*), the relative expression levels of *agrB*,  
293 *agrD* and *agrC* were significantly lower (n=3, P<0.05) than those of the parental strain EGD-  
294 e (Fig. 4B). Indeed, the relative transcript levels for *agrB*, *agrD* and *agrC* were respectively

295 of 56, 68 and 3 fold lower than those measured with the parental strain. A similar pattern of  
296 gene expression was observed for mutant DG119D ( $\Delta agrD$ ) (Fig. 4B). In terms of the relative  
297 expression levels of *agrA*, no significant differences were observed between the mutants  
298 (DG119D and DG125A) and parental strains. These results suggest an autoregulation of the  
299 transcription of *agrB*, *agrD* and *agrC* and a low constitutive expression of the putative  
300 transcriptional regulator AgrA.

301 The mRNA quantification data suggested that the *agr* system was autoregulated and pointed  
302 to a differential expression of the *agr* genes during sessile and planktonic growth. Either post  
303 transcriptional processing or transcription from another promoter region, not yet identified,  
304 could account for these results.

#### 305 **Processing of the mRNA and identification of the 5' end of the mRNA *agr* operon**

306 In order to further investigate the hypothesis of a processing, RT-PCR, Northern blotting and  
307 mRNA chemical half-life were carried out. The four genes and the two intergenic regions  
308 were detected by RT-PCR (Fig. 5), indicating cotranscription of the complete *agrBDCA*  
309 operon and the presence of a full-size transcript. PCR on the RNA samples before reverse  
310 transcription gave no amplification signals, confirming that there was no contamination by  
311 genomic DNA (data not shown). However, a polycistronic mRNA was never detected by  
312 Northern blotting but only small size products (data not shown). The mRNA chemical half-  
313 life was determined using real time PCR experiments with the same primer sets as above (Fig.  
314 1A, Table 2). Results indicated that the chemical half-life of *agrB* and *agrD* transcripts was  
315 7.4 and 6.8 min respectively, while it was lower for *agrC* and *agrA* (4.3 min and 4.1 min  
316 respectively) (Fig. 6). To pinpoint these differences in chemical half-life and to highlight the  
317 differential expression pattern observed by real time PCR, 5'RACE experiments were carried  
318 out to search for transcription initiation points or cleavages within *agrC* and *agrA* transcripts.  
319 Regardless of the treatment with TAP, multiple PCR products were detected, confirming

320 degradation after cleavage through RNase activity. After amplification with adequate primers  
321 (Table 2), four 5' ends were identified among the *agrC* fragments sequenced (Fig. 7).  
322 Similarly, five 5' ends were observed among the *agrA* fragments sequenced (Fig. 7). From  
323 two hypotheses formulated, data analysis confirmed post-transcriptional cleavage and  
324 degradation.

325 5' RACE was also used to characterize the 5' end of the mRNA *agr* operon. PCR  
326 amplification was observed in TAP-treated and untreated samples, suggesting a processing  
327 event at the 5' end, mapped by a "T" (Fig. 7). As expected, primer extension analysis with the  
328 three specific primers B34, B26 and B18 (Table 2) revealed two signals. They were separated  
329 by one nucleotide and corresponded to a "G" and the previously described "T". This finding  
330 suggested that the 5' end of the *agr* transcript was located 15 or 14 nucleotides upstream from  
331 the putative start codon (Fig. 7). Similar results were obtained in samples harvested at OD<sub>600</sub>  
332 of 0.1, 0.4 and 0.6. Moreover, two hexanucleotides (TGGTTA and TAAAAT) separated by  
333 18 nucleotides were detected upstream. They presented similarities to the consensus -35 and  
334 -10 sequences of several promoters of housekeeping genes from Gram positive bacteria as  
335 well as from *E. coli* (21, 23). Sequence conservation is higher in the -10 region than in the -  
336 35 region, and a TGn extension was observed upstream of the -10 region. Similar features  
337 were found in several promoters of Gram positive bacteria (20, 38).

338

339

## 340 **DISCUSSION**

341

342 Orthologs of the *agr* system, initially described in *S. aureus*, have been reported in  
343 *L. plantarum*, *E. faecalis* and *L. monocytogenes* (6, 44, 48, 56). So far, the role of the *agr*  
344 system has not been clearly described in the pathogenic bacterium *L. monocytogenes*. In this  
345 study, we investigated the role of *agrA* and *agrD* in the sessile growth of *L. monocytogenes*  
346 and we focussed on the molecular characterization of the transcription of the *agr* operon. In-  
347 frame deletions of *agrA*, that encodes a transcriptional regulator, or in-frame deletions of  
348 *agrD* encoding a propeptide affected adhesion and the early stages of biofilm formation on  
349 glass and polystyrene surfaces within the first 24 h of incubation. No significant differences  
350 were observed afterwards. These results are in accordance with those obtained by Sturme *et*  
351 *al.* (48) with a *lamA* mutant of *L. plantarum* WCFS1. Indeed, the *lamA* mutant was impaired  
352 in its ability to adhere to glass surfaces. It showed a 1.5-fold and 1.7-fold decrease in glass  
353 adherence compared to the parental strain after 24 and 48 h respectively. In contrast, Vuong *et*  
354 *al.* (52), working with *S. aureus* RN6390 and 601055, demonstrated that their *agr*<sup>-</sup> genotype  
355 led to a pronounced attachment to polystyrene, 1.8-fold and 2.5-fold increase respectively  
356 compared to that of the isogenic *agr*<sup>+</sup> wild type after 24 h. Biofilm-associated infections have  
357 special clinical relevance and in staphylococcal infections, these diseases include  
358 endocarditis, osteomyelitis, implanted device-related infections, and even some skin  
359 infections (54). Indeed, the *agr*<sup>-</sup> biofilm phenotype may have important consequences. For  
360 example, the dysfunction of *agr* is correlated with persistent bacteremia in *S. aureus* (49) and  
361 mutation of *S. aureus agr* system increased bacterial persistence (52), suggesting that  
362 interference with cell-cell communication would enhance rather than suppress this important  
363 type of staphylococcal disease (42).

364 In our experimental conditions, growth phase-dependent transcriptional regulation was not

365 observed during planktonic growth. This is in agreement with a previous report which showed  
366 that during exponential and stationary phases, the amount of *agrB* and *agrC* mRNAs was not  
367 significantly different (6), although a twofold difference in the quantity of *agrA* transcripts  
368 was recorded by these authors. In contrast, the transcription of the orthologous *agr*, *lam* and  
369 *fsr* operons from *S. aureus* MN NJ, *L. plantarum* WCFS1 and *E. faecalis* OG1RF  
370 respectively, increased from early to mid-exponential phase, suggesting growth phase-  
371 dependent transcription up-regulation (44, 48, 56).

372 During sessile growth, the transcription of the *agr* genes depended on the stage of biofilm  
373 development, suggesting that this system is important during biofilm development.  
374 Interestingly, a significant decrease in the transcript levels of *agrB*, *agrD* and *agrC* was  
375 observed following initial attachment. At first glance, this may seem surprising as initial  
376 attachment is the step where *agr* impairment is most detrimental to biofilm formation ; this  
377 points out that developmental regulations involved during sessile growth are complex (22). In  
378 *L. monocytogenes*, *agr*-dependent regulation may be transitory during biofilm formation as  
379 was observed in other systems. For example, two communication systems (*las* and *rhl*) play a  
380 role in transitional episodes in *Pseudomonas aeruginosa* biofilm development. The Las  
381 regulon is involved in early biofilm development but not in later stages; on the opposite, the  
382 Rhl regulon plays a role in maturation of the biofilm (14, 46). The *agr* system of *L.*  
383 *monocytogenes* could also regulate the expression of proteins necessary for the ability to  
384 attach to abiotic surfaces without being involved once the cells attach to the surface. Indeed,  
385 in *S. aureus* and *S. epidermidis*, *agr*-dependent regulation of the expression of several  
386 adhesion proteins has been demonstrated (12, 34).

387 Significant differences were measured in the relative quantities of the transcripts of *agrB*,  
388 *agrD*, *agrC* and *agrA*, while the differences between the transcripts of *agrB* and *agrD* were  
389 never significantly different. This observation suggested either post transcriptional processing

390 of the full-size *agr* transcript of *L. monocytogenes* or the presence of another promoter region  
391 between *agrD* and *agrC*. Determination of 5' ends corresponding to cleavage, and not to an  
392 initiation transcription points, supported the post transcriptional events hypothesis. Indeed,  
393 several 5' ends were detected within *agrC* and *agrA* transcripts. This suggested also that most  
394 of the transcripts quantified by real time PCR were degradation products generated after  
395 cleavage of the full-length transcript, probably within the intergenic region or at the 5' end of  
396 *agrC* and *agrA*. These post-transcriptional events may have regulatory functions resulting in a  
397 differential stability and a rapid processing of the mRNA. This could account for a fine tuning  
398 of the expression of the individual genes of the *agr* operon as has previously been suggested  
399 for the pattern of expression of other loci of Gram-negative and Gram-positive bacteria (2, 24,  
400 25, 37, 40 ). Moreover, our work indicated that the *agr* operon of *L. monocytogenes* was  
401 autoregulated in a positive way since the deletion of *agrA* or *agrD* reduced the transcription  
402 of *agrB*, *agrD* and *agrC*, although *agrA* transcription was not *agr* dependent. A similar  
403 pattern has been described in the orthologous *fsr* system of *E. faecalis* in which expression of  
404 *fsrB*, *fsrD* and *fsrC* are *fsr* dependent, while expression of the *fsrA* is weak, constitutive and  
405 *fsr*-independent (29, 45). It is proposed, in one hand, that the regulator is constitutively  
406 expressed in order to provide a basal amount of regulator ready to respond to the presence of  
407 the signal in the environment of the cell ; on the other hand, when the signal is high in the  
408 environment of the cell, it would induce the expression of the transmembrane protein, the  
409 propeptide and the sensor ; this in turn would enable the transfer of the signal to the  
410 neighbouring cells and prepare the cell to the monitoring of an amplified signal (18, 26).

411 Two 5' ends of the *agr* mRNA were determined. One was mapped to a "G" and located at an  
412 appropriate distance downstream of the putative promoter region (43), leading us to consider  
413 it as the apparent start site for the promoter of the *agr* operon. The second 5' end identified  
414 was located one base downstream of the 5' end of the primary transcript. Such cleavage of

415 one nucleotide downstream of the initiation site may derive from a modification of the  
416 primary transcript by a phosphatase or pyrophosphatase, or from endonucleolytic cleavage  
417 (31, 47, 50, 51). The significance of such commonly observed processing remains to be  
418 clarified.

419 In conclusion, this study is the first description of the involvement of cell-cell communication  
420 on adherence of *L. monocytogenes*. Our data showed that impairment of the response  
421 regulator or the propeptide resulted in a similarly altered adhesion and biofilm phenotype. The  
422 *agr* system of *L. monocytogenes* differed from the homologous systems previously described  
423 as post transcriptional processing occurred at the site of initiation of transcription and within  
424 the full-length transcript. It will be of interest to investigate the significance of such a  
425 processing in the expression of the *agr* system and in the physiology of *L. monocytogenes*.

426

427

428 **ACKNOWLEDGEMENTS**

429 This work was supported by the Ministère de l'Education Nationale de la Recherche et de la  
430 Technologie, the Université de Bourgogne and the Institut National de la Recherche  
431 Agronomique. We thank Dr. Sofia Kathariou for providing the pGF-EM vector, Dr. Philippe  
432 Gaudu for his critical reading of this manuscript and Mary Boulay for her reading of the  
433 English text.

434

435

437

- 438 1. **Aguado, V., A. I. Vitas, and I. Garcia-Jalon.** 2004. Characterization of *Listeria monocytogenes* and  
439 *Listeria innocua* from a vegetable processing plant by RAPD and REA. *Int. J. Food Microbiol.* **90**:341-  
440 347.
- 441 2. **Allenby, N. E. E., N. O'Connor, Z. Pragai, N. M. Carter, M. Miethke, S. Engelmann, M. Hecker,**  
442 **A. Wipat, A. C. Ward, and C. R. Harwood.** 2004. Post-transcriptional regulation of the *Bacillus*  
443 *subtilis* *pst* operon encoding a phosphate-specific ABC transporter. *Microbiology* **150**:2619-2628.
- 444 3. **Allison, D. G., B. Ruiz, C. SanJose, A. Jaspe, and P. Gilbert.** 1998. Extracellular products as  
445 mediators of the formation and detachment of *Pseudomonas fluorescens* biofilms. *FEMS Microbiol.*  
446 *Lett.* **167**:179-184.
- 447 4. **Arvidson, S., and K. Tegmark.** 2001. Regulation of virulence determinants in *Staphylococcus aureus*.  
448 *Int. J. Med. Microbiol.* **291**:159-170.
- 449 5. **Auger, S., E. Krin, S. Aymerich, and M. Gohar.** 2006. Autoinducer 2 affects biofilm formation by  
450 *Bacillus cereus*. *Appl. Environ. Microbiol.* **72**:937-941.
- 451 6. **Autret, N., C. Raynaud, I. Dubail, P. Berche, and A. Charbit.** 2003. Identification of the *agr* locus  
452 of *Listeria monocytogenes*: role in bacterial virulence. *Infect. Immun.* **71**:4463-4471.
- 453 7. **Balestrino, D., J. A. J. Haagenen, C. Rich, and C. Forestier.** 2005. Characterization of type 2  
454 quorum sensing in *Klebsiella pneumoniae* and relationship with biofilm formation. *J. Bacteriol.*  
455 **187**:2870-2880.
- 456 8. **Bassler, B. L.** 2002. Small talk: cell-to-cell communication in bacteria. *Cell* **109**:421-424.
- 457 9. **Bensing, B. A., B. J. Meyer, and G. M. Dunny.** 1996. Sensitive detection of bacterial transcription  
458 initiation sites and differentiation from RNA processing sites in the pheromone-induced plasmid  
459 transfer system of *Enterococcus faecalis*. *Proc. Natl. Acad. Sci.* **93**:7794-7799.
- 460 10. **Bergmann, B., D. Raffelsbauer, M. Kuhn, M. Goetz, S. Hom, and W. Goebel.** 2002. InlA- but not  
461 InlB-mediated internalization of *Listeria monocytogenes* by non-phagocytic mammalian cells needs the  
462 support of other internalins. *Mol. Microbiol.* **43**:557-570.
- 463 11. **Challan Belval, S., L. Gal, S. Margiewes, D. Garmyn, P. Piveteau, and J. Guzzo.** 2006. Assessment  
464 of the roles of LuxS, S-Ribosyl homocysteine, and autoinducer 2 in cell attachment during biofilm  
465 formation by *Listeria monocytogenes* EGD-e. *Appl. Environ. Microbiol.* **72**:2644-2650.
- 466 12. **Cramton, S. E., C. Gerke, N. F. Schnell, W. W. Nichols, and F. Gotz.** 1999. The Intercellular  
467 Adhesion (*ica*) Locus Is Present in *Staphylococcus aureus* and Is Required for Biofilm Formation.  
468 *Infect. Immun.* **67**:5427-5433.
- 469 13. **Crossman, L., and J. M. Dow.** 2004. Biofilm formation and dispersal in *Xanthomonas campestris*.  
470 *Microbes Infect.* **6**:623-629.
- 471 14. **Davies, D. G., Parsek, M.R., Pearson, J.P., Iglewski, B.H., Costerton, J.W., Greenberg, E.P.** 1998.  
472 The involvement of cell-to-cell signals in the development of bacterial biofilm. *Science* **280**:295-298.
- 473 15. **Desroche, N., C. Beltramo, and J. Guzzo.** 2005. Determination of an internal control to apply reverse  
474 transcription quantitative PCR to study stress response in the lactic acid bacterium *Oenococcus oeni*. *J.*  
475 *Microbiol. Meth.* **60**:325-333.
- 476 16. **Djordjevic, D., M. Wiedmann, and L. A. McLandsborough.** 2002. Microtiter plate assay for  
477 assessment of *Listeria monocytogenes* biofilm formation. *Appl. Environ. Microbiol.* **68**:2950-2958.
- 478 17. **Donlan, R. M., and J. W. Costerton.** 2002. Biofilms: survival mechanisms of clinically relevant  
479 microorganisms. *Clin. Microbiol. Rev.* **15**:167-193.
- 480 18. **Dunn, A. K., and E. V. Stabb.** 2007. Beyond quorum sensing : the complexities of prokaryotic  
481 parliamentary procedures. *Anal. Bioanal. Chem.* **387**:391-398.
- 482 19. **Farber, J. M. a. P., P.I.** 1991. *Listeria monocytogenes*, a food-borne pathogen. *Microbiol. Rev.*  
483 **55**:476-511.
- 484 20. **Garmyn, D., T. Ferain, N. Bernard, P. Hols, and J. Delcour.** 1995. Cloning, nucleotide sequence,  
485 and transcriptional analysis of the *Pediococcus acidilactici* L-(+)-lactate dehydrogenase gene. *Appl.*  
486 *Environ. Microbiol.* **61**:266-272.
- 487 21. **Guzzo, J., M.-P. Jobin, F. Delmas, L.-C. Fortier, D. Garmyn, R. Tourdot-Marechal, B. Lee, and**  
488 **C. Divies.** 2000. Regulation of stress response in *Oenococcus oeni* as a function of environmental  
489 changes and growth phase. *Int. J. Food Microbiol.* **55**:27-31.
- 490 22. **Hall-Stoodley, L., and P. Stoodley.** 2002. Developmental regulation of microbial biofilms. *Curr. Opin.*  
491 *Biotechnol.* **13**:228-233.
- 492 23. **Harley, C. B., and R. P. Reynolds.** 1987. Analysis of *E. coli* promoter sequences. *Nucl. Acids Res.*  
493 **15**:2343-2361.

- 494 24. **Hebermehl, M., and G. Klug.** 1998. Effect of oxygen on translation and posttranslational steps in  
495 expression of photosynthesis genes in *Rhodobacter capsulatus*. *J. Bacteriol.* **180**:3983-3987.
- 496 25. **Homuth, G., A. Mogk, and W. Schumann.** 1999. Post-transcriptional regulation of the *Bacillus*  
497 *subtilis dnaK* operon. *Mol. Microbiol.* **32**:1183-1197.
- 498 26. **Horswill, A. R., P. Stoodley, P. S. Stewart, and M. R. Parsek.** 2007. The effect of the chemical,  
499 biological, and physical environment on quorum sensing in structured microbial communities. *Anal.*  
500 *Bioanal. Chem.* **387**:371-380.
- 501 27. **Huber, B., K. Riedel, M. Hentzer, A. Heydorn, A. Gotschlich, M. Givskov, S. Molin, and L. Eberl.**  
502 2001. The *cep* quorum-sensing system of *Burkholderia cepacia* H111 controls biofilm formation and  
503 swarming motility. *Microbiology* **147**:2517-2528.
- 504 28. **Jefferson, K. K.** 2004. What drives bacteria to produce a biofilm? *FEMS Microbiol. Lett.* **236**:163-173.
- 505 29. **Ji, G., R. C. Beavis, and R. P. Novick.** 1995. Cell density control of staphylococcal virulence  
506 mediated by an octapeptide pheromone. *Proc. Natl. Acad. Sci.* **92**:12055-12059.
- 507 30. **Kjelleberg, S., and S. Molin.** 2002. Is there a role for quorum sensing signals in bacterial biofilms?  
508 *Curr. Opin. Microbiol.* **5**:254-258.
- 509 31. **Kühn, K., A. Weihe, and T. Börner.** 2005. Multiple promoters are a common feature of mitochondrial  
510 genes in *Arabidopsis*. *Nucl. Acids Res.* **33**:337-346.
- 511 32. **Lawrence, L., and A. Gilmour.** 1995. Characterization of *Listeria monocytogenes* isolated from  
512 poultry products and from the poultry-processing environment by random amplification of polymorphic  
513 DNA and multilocus enzyme electrophoresis. *Appl. Environ. Microbiol.* **61**:2139-2144.
- 514 33. **Li, G., and S. Kathariou.** 2003. An improved cloning vector for construction of gene replacements in  
515 *Listeria monocytogenes*. *Appl. Environ. Microbiol.* **69**:3020-3023.
- 516 34. **Mack, D., A. P. Davies, L. G. Harris, H. Rohde, M. A. Horstkotte, and J. K. M. Knobloch.** 2007.  
517 Microbial interactions in *Staphylococcus epidermidis* biofilms. *Anal. Bioanal. Chem.* **387**:399-408.
- 518 35. **McNab, R., S. K. Ford, A. El-Sabaeny, B. Barbieri, G. S. Cook, and R. J. Lamont.** 2003. LuxS-  
519 Based signaling in *Streptococcus gordonii*: Autoinducer 2 controls carbohydrate metabolism and  
520 biofilm formation with *Porphyromonas gingivalis*. *J. Bacteriol.* **185**:274-284.
- 521 36. **Merritt, J., F. Qi, S. D. Goodman, M. H. Anderson, and W. Shi.** 2003. Mutation of *luxS* affects  
522 biofilm formation in *Streptococcus mutans*. *Infect. Immun.* **71**:1972-1979.
- 523 37. **Mongkolsuk, S., W. Panmanee, S. Atichartpongkul, P. Vattanaviboon, W. Whangsuk, M.**  
524 **Fuangthong, W. Eiamphungporn, R. Sukchawalit, and S. Utamapongchai.** 2002. The repressor for  
525 an organic peroxide-inducible operon is uniquely regulated at multiple levels. *Mol. Microbiol.* **44**:793-  
526 802.
- 527 38. **Murakami, S. K., S. Masuda, E. A. Campbell, O. Muzzin, and S. A. Darst.** 2002. Structural basis of  
528 transcription initiation: an RNA polymerase holoenzyme-DNA complex. *Science* **296**:1285-1290.
- 529 39. **Murray, E. G. D., Webb, R.A. and Swann, M.B.R.** 1926. A disease of rabbit characterised by a large  
530 mononuclear leucocytosis, caused by a hitherto undescribed bacillus: *Bacterium monocytogenes*. *J.*  
531 *Pathol. Bacteriol.* **29**:407-439.
- 532 40. **Nilsson, P., S. Naureckiene, and B. Uhlin.** 1996. Mutations affecting mRNA processing and fimbrial  
533 biogenesis in the *Escherichia coli pap* operon. *J. Bacteriol.* **178**:683-690.
- 534 41. **Novick, R. P., S. J. Projan, J. Kornblum, H. F. Ross, G. Ji, B. Kreiswirth, F. Vandenesch, and S.**  
535 **Moghazeh.** 1995. The *agr* P2 operon: an autocatalytic sensory transduction system in *Staphylococcus*  
536 *aureus*. *Mol. Gen. Genet.* **248**:446-458.
- 537 42. **Otto, M.** 2004. Quorum-sensing control in Staphylococci-a target for antimicrobial drug therapy?  
538 *FEMS Microbiol. Lett.* **241**:135-141.
- 539 43. **Phadtare, S., and K. Severinov.** 2005. Extended -10 motif is critical for activity of the *cspA* promoter  
540 but does not contribute to low-temperature transcription. *J. Bacteriol.* **187**:6584-6589.
- 541 44. **Qin, X., K. V. Singh, G. M. Weinstock, and B. E. Murray.** 2001. Characterization of *fsr*, a regulator  
542 controlling expression of gelatinase and serine protease in *Enterococcus faecalis* OG1RF. *J. Bacteriol.*  
543 **183**:3372-3382.
- 544 45. **Qin, X., K. V. Singh, G. M. Weinstock, and B. E. Murray.** 2000. Effects of *Enterococcus faecalis fsr*  
545 genes on production of gelatinase and a serine protease and virulence. *Infect. Immun.* **68**:2579-2586.
- 546 46. **Sauer, K., A. K. Camper, G. D. Ehrlich, J. W. Costerton, and D. G. Davies.** 2002. *Pseudomonas*  
547 *aeruginosa* displays multiple phenotypes during development as a biofilm. *J. Bacteriol.* **184**:1140-1154.
- 548 47. **Silvaggi, J. M., J. B. Perkins, and R. Losick.** 2005. Small untranslated RNA antitoxin in *Bacillus*  
549 *subtilis*. *J. Bacteriol.* **187**:6641-6650.
- 550 48. **Sturme, M. H. J., J. Nakayama, D. Molenaar, Y. Murakami, R. Kunugi, T. Fujii, E. E. Vaughan,**  
551 **M. Kleerebezem, and W. M. de Vos.** 2005. An *agr*-like two-component regulatory system in  
552 *Lactobacillus plantarum* is involved in production of a novel cyclic peptide and regulation of  
553 adherence. *J. Bacteriol.* **187**:5224-5235.

- 554 49. **Vance G. Fowler, J., G. Sakoulas, L. M. McIntyre, V. G. Meka, R. D. Arbeit, C. H. Cabell, M. E.**  
555 **Stryjewski, G. M. Eliopoulos, L. B. Reller, G. R. Corey, T. Jones, N. Lucindo, M. R. Yeaman, and**  
556 **A. S. Bayer.** 2004. Persistent bacteremia due to methicillin-resistant *Staphylococcus aureus* infection is  
557 associated with *agr* dysfunction and low-level in vitro resistance to thrombin-induced platelet  
558 microbicidal protein. *J. Infect. Dis.* **190**:1140-1149.
- 559 50. **Vogel, J., I. M. Axmann, H. Herzel, and W. R. Hess.** 2003. Experimental and computational analysis  
560 of transcriptional start sites in the *Cyanobacterium Prochlorococcus* MED4. *Nucl. Acids Res.* **31**:2890-  
561 2899.
- 562 51. **Vogel, J., V. Bartels, T. H. Tang, G. Churakov, J. G. Slagter-Jäger, A. Hüttenhofer, E. Gerhart,**  
563 **and H. Wagner.** 2003. RNomics in *Escherichia coli* detects new sRNA species and indicates parallel  
564 transcriptional output in bacteria. *Nucl. Acids Res.* **31**:6435-6443.
- 565 52. **Vuong, C., Saenz, H L, Gotz, F, Otto, M.** 2000. Impact of the *agr* quorum-sensing system on  
566 adherence to polystyrene in *Staphylococcus aureus*. *J. Infect. Dis.* **182**:1688-1693.
- 567 53. **Williams, T., S. Bauer, D. Beier, and M. Kuhn.** 2005. Construction and characterization of *Listeria*  
568 *monocytogenes* mutants with in-frame deletions in the response regulator genes identified in the  
569 genome sequence. *Infect. Immun.* **73**:3152-3159.
- 570 54. **Xu, L., H. Li, C. Vuong, V. Vadyvaloo, J. Wang, Y. Yao, M. Otto, and Q. Gao.** 2006. Role of the  
571 *luxS* quorum-sensing system in biofilm formation and virulence of *Staphylococcus epidermidis*. *Infect.*  
572 *Immun.* **74**:488-496.
- 573 55. **Yarwood, J. M., D. J. Bartels, E. M. Volper, and E. P. Greenberg.** 2004. Quorum sensing in  
574 *Staphylococcus aureus* biofilms. *J. Bacteriol.* **186**:1838-1850.
- 575 56. **Yarwood, J. M., J. K. McCormick, M. L. Paustian, V. Kapur, and P. M. Schlievert.** 2002.  
576 Repression of the *Staphylococcus aureus* accessory gene regulator in serum and in vivo. *J. Bacteriol.*  
577 **184**:1095-1101.
- 578 57. **Yarwood, J. M., and P. M. Schlievert.** 2003. Quorum sensing in *Staphylococcus* infections. *J. Clin.*  
579 *Invest.* **112**:1620-1625.
- 580  
581

582 TABLE 1. Bacterial strains and plasmids used in this study

Bacterial strain or plasmid	Relevant property <sup>a</sup>	Reference or source
<i>E. coli</i> TOP10	Cloning host	Invitrogen
<i>E. coli</i> Match1	Cloning host	Invitrogen
<i>L. monocytogenes</i> EGD-e	Wild type of serotype 1/2a for which the genome sequence is available	(39)
<i>L. monocytogenes</i> DG125A	<i>L. monocytogenes</i> EGD-e with in-frame deletion of <i>agrA</i> gene	This work
<i>L. monocytogenes</i> DG119D	<i>L. monocytogenes</i> EGD-e with in-frame deletion of <i>agrD</i> gene	This work
pGF-EM	Cm <sup>r</sup> Am <sup>r</sup> ; 9.4-kb derivative of pCON-1 containing 0.8-kb <i>gfp</i> gene of pKV111 and <i>erm</i> gene of Tn917	(33)
pGID109	Km <sup>r</sup> Am <sup>r</sup> ; 4.4-kb derivative of pCR21- TOPO containing 0.6-kp 3'end of <i>agrD</i> and 5'end of <i>agrC</i>	This work
pGID112	Cm <sup>r</sup> Am <sup>r</sup> ; 10.4-kb derivative of pGF-EM containing 0.4-kb 5'end of <i>agrD</i>	This work
pGID118	Km <sup>r</sup> Am <sup>r</sup> ; 4.3-kb derivative of pCR21- TOPO containing 0.5-kp internal region of <i>agrA</i>	This work
pGID119	Cm <sup>r</sup> Am <sup>r</sup> ; 9.4-kb derivative of pGID112 containing 3'end of <i>agrD</i> inserted into XbaI/EcoRI site of pGID109	This work
pGID121	Cm <sup>r</sup> Am <sup>r</sup> ; 10.6-kb derivative of pGF-EM containing 0.6-kb 3'end of <i>agrC</i> and ATG of <i>agrA</i>	This work
pGID125	Cm <sup>r</sup> Am <sup>r</sup> ; 9.3-kb derivative of pGID121 containing internal region of <i>agrA</i> inserted into XbaI/EcoRI site of pGID118	This work

583 <sup>a</sup> Km<sup>r</sup>, kanamycin resistant ; Am<sup>r</sup>, ampicillin resistant ; Cm<sup>r</sup>, chloramphenicol resistant.

584

585

586 TABLE 2. Oligonucleotides used in this study

Description and application	Sequence (5'→3') <sup>a</sup>	Created restriction site	Primers name
<u>Constructions</u>			
pGID121	<b>AAAGCTT</b> CGCGTTTTTCGTCATGATT <b>ATCTAGAC</b> CATAAATTCATCCCCATTCT	HindIII XbaI	C13 A12
pGID118	<b>AGCTAGCA</b> ACAGGAGATCCGTTTGAG CTTACCATAAAAATTCCACTT	NheI	A15 E2
pGID112	CAA <b>AGCTTTT</b> ACTGCAAACA AAGAATCCGCAACTTTCATGG	HindIII	D1 D2
pGID109	CTATGAGT <b>CTAGATT</b> GCTTCATG AACAAATTCGCCAACATTCC	XbaI	D3 D4
<u>RNA analysis</u>			
qRT-PCR <i>drm</i>	GCGGAAAAACCACTTGCTTACT CGGAAAGGTGTGTCAATGTATAGG		DRMF2 DRMR2
qRT-PCR <i>agrB</i>	CGGCAGACACAGAAAGTTTG TGCGAATGGTATTAGCAACG		BF2 BR2
qRT-PCR <i>agrD</i>	AAATCAGTTGGTAAATTCCTTTCTAG AATGGACTTTTTGGTTCGTATACA		DF2 DR2
qRT-PCR <i>agrC</i>	GGGGTCAATCGCAGGTTTTG CTTTAAGTTCGTTGGTTGCCGTA		CF2 CR2
qRT-PCR <i>agrA</i>	GCAAGCAGAAGAACGATTTCCAA CGCTGTCTCAAAAAACAAGATAT		AF2 AR2
RT-PCR <i>agrBD</i>	CAA <b>AGCTTTT</b> ACTGCAAACA TTGCATTTTCACAAATGGACTT	HindIII	D1 DR
RT-PCR <i>agrDC</i>	CCATGAAAGTTGCGGATTCT GGCACTTACAAAAACAATCAATAC		DF C35
RT-PCR <i>agrC</i> and Northern blot <i>agrC</i>	GGAATGTTGGCGAATTTGTT CTTCAAACCCGGCATATCAT		C11 C10
RT-PCR <i>agrCA</i>	CAAAAGGAGAAGGTCGTGGA ACCATTCATGTCCGGCTGCC		C23 A46
Northern blot <i>agrB</i>	<b>ACCATGGG</b> TAAATTCGTTGTAAAATA CGTGCAATTCAATGTTTTGG	NcoI	B17 BR
Northern blot <i>agrA</i>	<b>AGCTAGCA</b> ACAGGAGATCCGTTTGAG CTTACCATAAAAATTCCACTT	NheI	A15 E2
5'RACE <i>agrB</i>	TGCGAATGGTATTAGCAACG CGAAATCAACACATCCGCCAT		BR2 B34
5'RACE <i>agrC</i>	GGCACTTACAAAAACAATCAATAC CTAAAGTAAATAAAGGGAAGGCTA		C35 C36
5'RACE <i>agrA</i>	TTGATGTGTAGGCATTTCGTG ACCATTCATGTCCGGCTGCC CGCTGCATTCTGTTATCTTCA CTTCAATATATTTTCGTTAACCT		A44 A46 A48 A50
Primer extension <i>agrB</i>	GACAAAGGGACTTTTGCAGT CTTCTTCATCATCTTCCAGCG CGAAATCAACACATCCGCCAT		B18 B26 B34

587 <sup>a</sup> Specific restriction sites are underlined and extra nucleotides added to include restriction sites to the PCR  
588 product are shown in bold type.  
589

590

591

592 **FIGURE LEGENDS**

593

594 FIG. 1. (A) Schematic diagram of *L. monocytogenes agr* operon. The grey arrows indicate the  
595 orientation and the size in base pairs of the four genes. Numbers between parentheses indicate  
596 the size in base pairs of the two intergenic regions. Arrowheads indicate the positions of the  
597 oligonucleotides used for real time PCR : b (BR2 ; BF2), d (DF2 ; DR2), c (CF2 ; CR2), a  
598 (AF2 ; AR2) and black lines indicate the probes used for Northern blotting (NB ; NC ; NA).  
599 The position of the transcription initiation site and the transcription termination site are  
600 indicated respectively by the bent arrow and the grey dot.

601 DNA and deduced amino acid sequence of (B) *agrA* gene containing a 106-bp deletion in  
602 DG125A ( $\Delta agrA$ ) mutant and of (C) *agrD* gene containing a 49-bp deletion in DG119D  
603 ( $\Delta agrD$ ) mutant. The position of the deletion is represented by an inverted black triangle, the  
604 nucleotides before and after the deletion are mentioned, the RBS are underlined, the start  
605 codons are boxed and the stop codon is represented by three stars.

606

607 FIG. 2. (A) *L. monocytogenes* EGD-e ■, DG125A ( $\Delta agrA$ ) ▒, and DG119D ( $\Delta agrD$ ) □ cell  
608 adhesion after 2 hours incubation at 25°C on glass slides. Histograms represent the number of  
609 adhered cells counted per microscopic field. Each bar indicates the mean of three independent  
610 experiments with four microscopic fields per experiment. (B) Micrographs of microscopic  
611 fields showing *L. monocytogenes* EGD-e, DG125A ( $\Delta agrA$ ) and DG119D ( $\Delta agrD$ ) cells  
612 adhering to glass slides after 2 hours incubation at 25°C. Magnification x 63.

613

614 FIG. 3. Biofilm formation by *L. monocytogenes* EGD-e ■, DG125A ( $\Delta agrA$ ) ▒, and  
615 DG119D ( $\Delta agrD$ ) □ in batch conditions in polystyrene 96-well plates after 16, 24, 48 and 72

616 hours incubation at 25°C. Each histogram indicates the mean of three independent  
617 experiments with five measurements for each point.

618

619 FIG. 4. Semilogarithmic representation of (A) relative expression levels of the *agrB*, *agrD*,  
620 *agrC* and *agrA* genes of the parental strain *L. monocytogenes* EGD-e determined during  
621 biofilm formation (2 hours □, 24 hours ▨ and 72 hours ▩) and planktonic growth (early  
622 exponential phase OD<sub>600</sub> of 0.1 ▤, mid exponential phase OD<sub>600</sub> of 0.4 ▥, stationary phase  
623 OD<sub>600</sub> of 0.6 ). (B) relative expression levels of the *agrB*, *agrD*, *agrC* and *agrA* genes of *L.*  
624 *monocytogenes* determined during mid exponential phase OD<sub>600</sub> of 0.4 (EGD-e strain ■,  
625 DG125A ( $\Delta agrA$ ) strain ▣, and DG119D ( $\Delta agrD$ ) strain □). For both graphs, gene  
626 expression was quantified using real time PCR and the comparative critical threshold ( $\Delta\Delta C_T$ )  
627 method. The *drm* gene was used as the internal standard, and expression of the *agrA* gene in  
628 the early exponential phase (OD<sub>600</sub> of 0.1) was used as the calibrator. Three independent  
629 experiments were performed; histograms indicate standard deviations.

630

631 FIG. 5. RT-PCR analysis of RNA from *L. monocytogenes* cells at mid exponential phase  
632 (OD<sub>600</sub> of 0.4). (A) The dotted lines enclosed by arrows indicate the positions of the primers  
633 and PCR products. (B) The amplified products, numbered 1 to 4, were separated by  
634 electrophoresis on 1% agarose gel and corresponded respectively to the expected size of 567,  
635 388, 435 and 353 base pairs. Sizes of the DNA marker fragments are notified in base pairs.

636

637 FIG. 6. Chemical half-life of the transcripts of the *agr* operon. Semilogarithmic plots of  
638 mRNA decay corresponding to *agrB* ■ *agrD* ◆ *agrC* ■ and *agrA* ▲ genes. Total RNA was  
639 prepared 0, 1, 4, 7 and 10 minutes after treatment with rifampicine (250  $\mu\text{g}\cdot\text{mL}^{-1}$ ). Results  
640 were obtained by real-time PCR analysis and normalized using 16S mRNA amounts. The

641 correlation coefficient ( $R^2$ ) and half life ( $T_{1/2}$ ) were determined for each regression analysis.

642 Three independent experiments were carried out.

643

644 FIG. 7. Analysis of the 5' end of *agrB*, *agrC* and *agrA* transcripts using total RNAs isolated

645 from EGD-e cells collected during the exponential growth phase ( $OD_{600}$  of 0.4). # indicates

646 the 5' end identified by primer extension and \* indicates processing sites identified by 5'

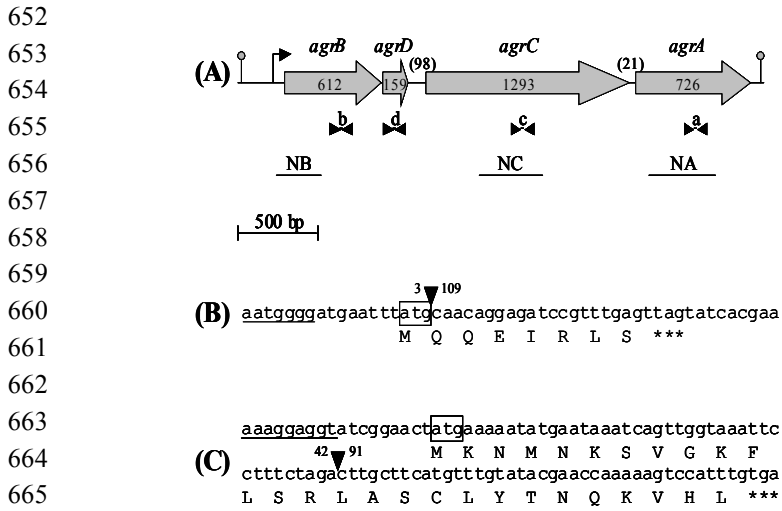
647 RACE. The putative -10 with TGn extension and -35 sequences are double underlined, the

648 RBS are underlined, the start codons are boxed and the stop codon of *agrC* is represented by

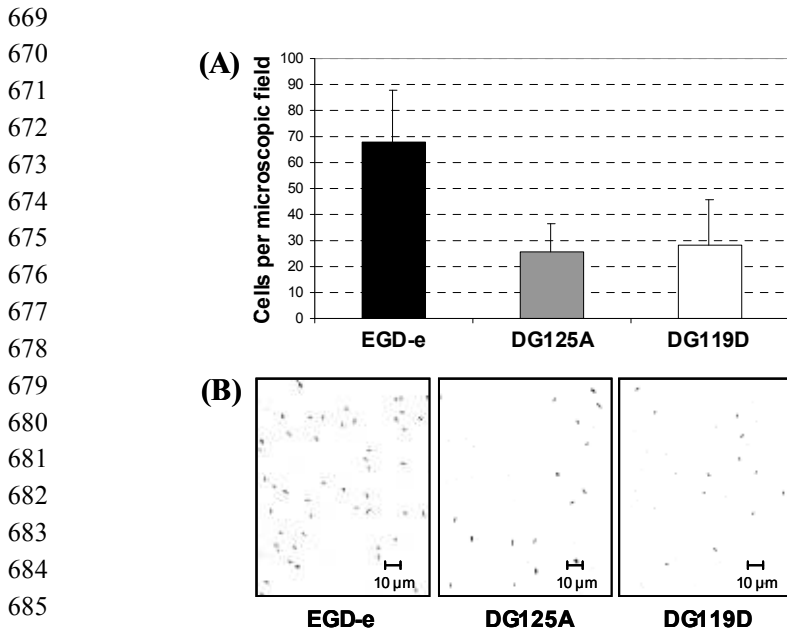
649 three stars.

650

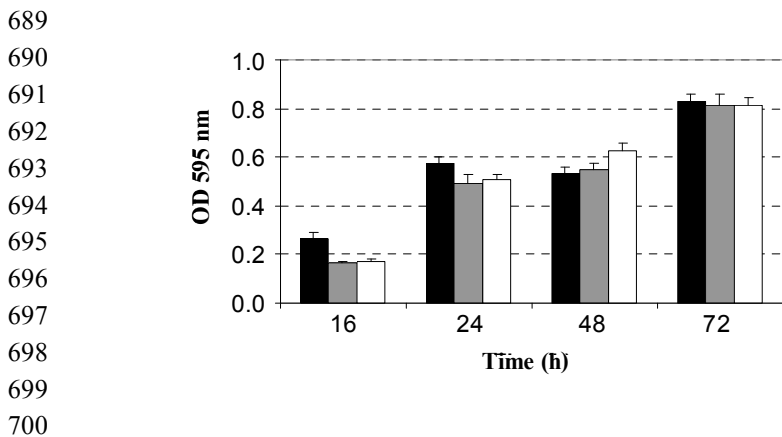
651 Fig.1



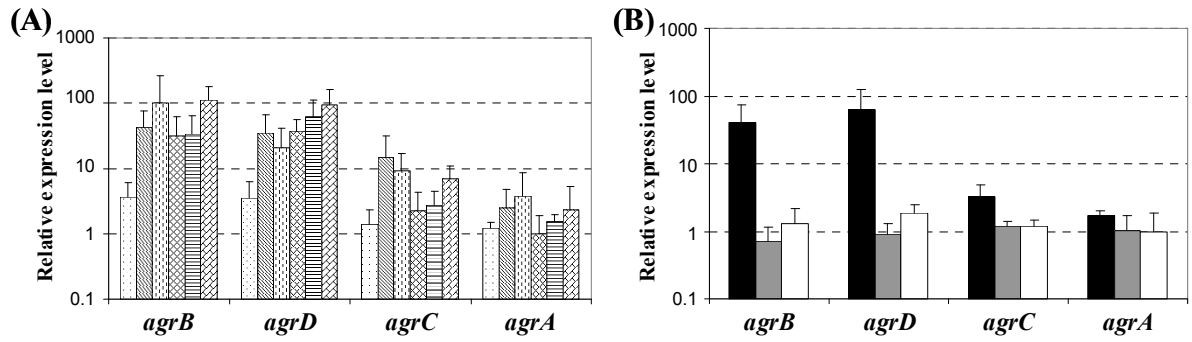
668 Fig. 2



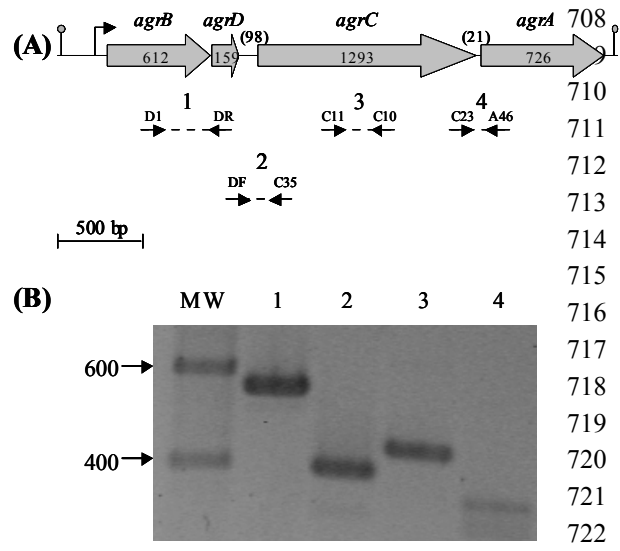
688 Fig. 3



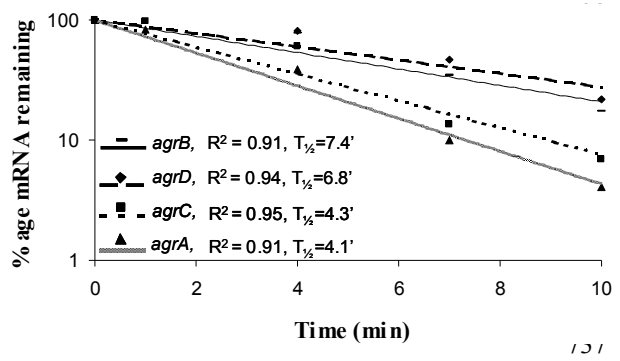
701 Fig. 4  
 702  
 703



704  
 705  
 706 Fig. 5  
 707



723  
 724  
 725  
 726 Fig. 6  
 727



738  
 739  
 740

741 Fig. 7  
742

**agrB** tacattttggttattatgggtaaaattcgttgtaaaatattagtgagggtgaattadttgagtaatttta ctgcaaagtcctttgtca  
M S N F T A K V P L S

**agrC** agaaggcaacttacatatttaaacatagatatttta gacagtgagggttaattatgttagtaattttga tggcaattatacagataacg  
M F S I L M A I I Q I T

ggtatttttattgcaatccagattttaa<sup>\*</sup>caaacaagtttttca<sup>\*</sup>attaaagagggatgggtactatagcaattgctatgctag<sup>\*</sup>ccttc  
G I F I A I Q I L T N K V F S I K E G L V T I A I A M L A F

**agrA** ggattaggccttgctagtttgcgggaaatta tgaagaatattcgcacgttgcttagatacgaagtgaccgatagagaagttattca<sup>\*</sup>  
G L G L A S L R E I M K K Y S H V A L D T K V T D R E V I Q

gaattagaaatta tgtagaagaatggggtg<sup>\*</sup>aatttatgctaccggttttattttgtgaagataacagaa tgcagcggagaaaggttaacg  
E L E I M \*\*\* M L P V F I C E D N R M Q R E R L T

aaatata ttgaagactata tta tggttgaacattttgata tgaagtagaac<sup>\*</sup>tttcaacaggagatccgtttgag<sup>\*</sup>ttag<sup>\*</sup>tatcacgaa tg  
K Y I E D Y I M V E H F D M K L E L S T G D P F E L V S R M

743  
744